2011 IEEE International Conference on
Automation Science and Engineering
Trieste, Italy - August 24-27, 2011

Weld Pool Visual Sensing without External Illumination

Jinchao Liu, Zhun Fan, *Senior Member, IEEE,* Søren Ingvor Olsen,
Kim Hardam Christensen, Jens Klæstrup Kristensen

***Abstract*— Visual sensing in arc welding has become more and more important, but still remains challenging because of the harsh environment with extremely strong illumination from the arc. This paper presents a low-cost camera-based sensor system, without using external Illumination, but nevertheless able to sense and model the weld pool. Central is a carefully selected optical filtering as well as an active contour-based tracking of the weld pool boundary. The system is able to extract the 2D shape of the weld pool in real time. The reported experiments show the feasibility of this approach.**

I. INTRODUCTION

The vast majority of the industrial welding work today is still being made manually due to the lack of closed-loop control of the arc welding process. This limits the productivity and the quality of the welding. Also it may harm the human welders by the airborne particles and gaseous by-products generated during welding. In the case of manually welding, the loop of the control system is closed by human welders observing the weld pool and the surrounding which can provide sufficient visual information to control the welding. This motivates researchers to develop visual sensors for the arc welding process.

Vision-based sensing is challenging due to the harsh environment including an extremely strong light from the arc. The arc is positioned directly above the weld pool making the latter almost invisible. One solution is to use a powerful external illumination to highlight the weld pool area and the surrounding. However, such systems are typically expensive and dangerous, therefore still used in a laboratory . To limit cost we prefer to use passive optical monocular vision with standard off-the-shelf equipment. This permits the vision system to be widely used in industrial environments.

This paper presents a low-cost machine vision system for closed-loop control in arc welding without external Illumination. The system is capable of observing the weld pool directly and extract the 2D shape of the weld pool in real time. By processing the extracted weld pool shapes, the dynamic of the weld pool may be modelled and used in an adaptive closed-loop control system. From the hardware side, the proposed machine vision system consists of a standard CCD camera and a combination of a bandpass filter and a neutral density filter to reduce the interference of the arc light. From the software side, we propose a novel visual tracking scheme based on active contour models to extract the 2D boundaries of the weld pool.

The rest of this paper is organized as follows. Section 2 summarizes previous work and section 3 presents the configuration of the proposed machine vision system, as well as the experiments platformIn section 4, the weld pool boundary tracking algorithm is presented. In section 5, we report the results of a real-time demonstration. Finally, section 6 concludes.

II. PREVIOUS WORK

During the last few decades an increasing focus on visual sensing in arc welding automation has been made. Brzakovic et al.[1] proposed a vision system which can determine the edges of the weld pool in images captured by a coaxial viewing system for gas-tungsten-arc welding processes. A tailored transform was used to map a weld pool edge into a vertical line. By detecting these lines in the transform domain, the weld pool edges were extractable. Abdullah et al.[2] developed a low-cost vision system for real time weld pool monitoring. A laser source was used to illuminate the weld area to overcome the presence of the welding arc. A low-cost CMOS camera was used for image acquisition. Precise synchronization between the camera and the short pulse laser made it possible to obtain high-quality images. Zhao et al.[3] proposed to estimate the three-dimensional parameters of weld pool for pulsed GTAW with wire filler from a single image using an improved shape from shading algorithm. Song et al.[4] used a dot-matrix pattern of laser light projected onto the weld pool surface. By analysing the distortion of the reflected dot-pattern, the surface of the weld pool could be recovered. Other research include [5], [6], [7].

To our knowledge, very few papers have reported the accurate tracking of the weld pool boundary without external illumination in real time. Most previous work either rely on external illumination or requires a significant amount of computations preventing real time performance. The importance of the accurate tracking of the weld pool as well as the surrounding is that it provides sufficient visual information for human welders to perform a quality welding. Based on the analysis of this information, it is possible to develop a fully-automated arc welding robot.

J. Liu is with Department of Management Engineering, Technical University of Denmark, 2800 lyngby, Denmark. He is also affiliated with FORCE Technology, 2650 Brønby, Denmark. jliu@man.dtu.dk

Z. Fan is with School of Electronics and Information Engineering,Tongji University, 200092, Shanghai, China. zfan@tongji.edu.cn

S. Olsen is with Department of Computer Science, University Of Copenhagen, 2100 Copenhagen, Denmark. ingvor@diku.dk

K. Christensen is with Division of Welding & Production Innovation, FORCE Technology, DK-2605 Brønby, Denmark. kmc@force.dk

J. Kristensen is with Division of Welding & Production Innovation, FORCE Technology, DK-2605 Brønby, Denmark. jek@force.dk

978-1-4577-1732-1/11/$26.00 ©2011 IEEE

III. System configuration

The proposed machine vision system, as well as the experimental platform is presented in Figure 1. The prototype vision system consists of an optical filtering system and an industrial b/w Prosilica GE 650 CCD camera produced by Allied Vision Technology.

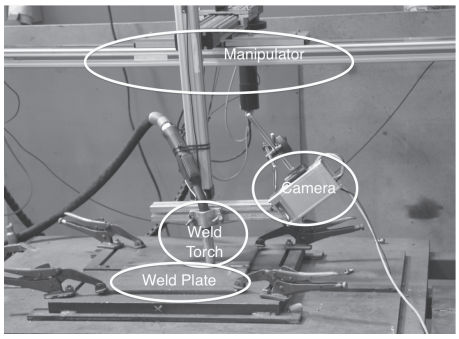

Fig. 1. The configuration of the experiments platform, including an industrial camera equipped with optical filters, a manipulator and a welding machine.

To reduce the interference of the high-intensity arc light a narrow band-pass filter with a center wavelength of 780 nm and a bandwidth of 10nm was used. In addition, a neutral density filter was also used to reduce the intensity of all kinds of lights and protect the bandpass filter from the spatters produced during welding.

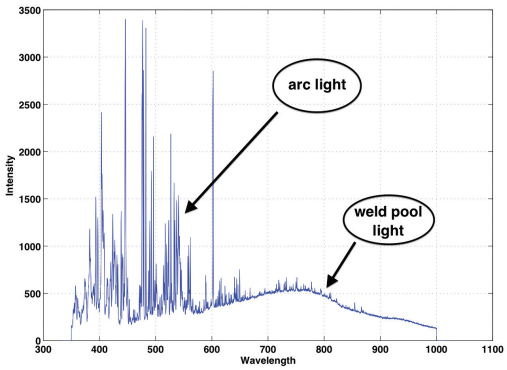

Fig. 2. The spectrum of the light generated during welding, including the weld pool light, the arc light.

The choice of band-pass filter was based on a spectrum analysis. Figure 2 shows the spectrum of the lights in a weld. It was captured by a spectrometer during welding. The exposure time of the spectrometer is 50ms. The distance from the optical probe of the spectrometer to the weld pool is approximately 10mm. It shows that the region in the spectrum that is mainly composed of the weld pool light is separate from the one of the arc light, in spite of that the intensity of the arc light is very high.

As shown in Figure 3 relatively high-quality images of the weld pool can be obtained using the procedure described above and a carefully selected exposure time. Next we need an algorithm to extract the weld pool boundary and to track this over time.

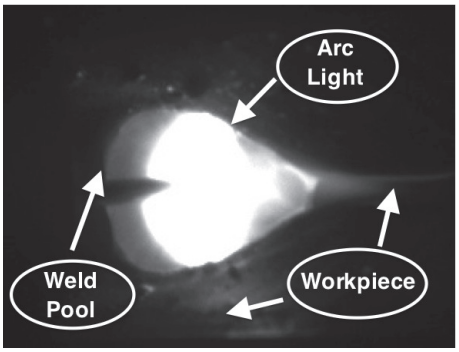

Fig. 3. The illustration of regions interested in this paper.

IV. Tracking the weld pool boundary

Although the weld pool boundary only develop slowly it is difficult to extract reliably because the arc light (escaping the optical filter system) varies a lot and because reflections may interfere. Thus, low-level approaches such as thresholding[8] or edge detection[9] do not perform satisfactorily. Often the strongest edges are not the correct ones and the detected edges do not form a closed contour. To achieve an acceptable result spacial and temporal consistency must be taken into account. Active contours, or snakes[10] offers an elegant framework where we may add prior knowledge and continuity constraints. Therefore, in this paper a visual tracking algorithm based on active contours was proposed to extract the weld pool boundary. Next section, we first review the original formulation of active contours and discuss two most relevant improvements.

A. Active contour models

Active contours[10] have been widely used in numerous applications. Mathematically, an active contour is a function or curve which minimizes an energy functional. Let Γ be a 1D curve which can be represented as

$$\boldsymbol{u}(s) = (x(s), y(s)), s \in [0, 1] \tag{1}$$

Then we may define the energy of this curve as follows:

$$E(\boldsymbol{u}) = \int_{\Gamma} \alpha \parallel \frac{d\boldsymbol{u}(s)}{ds} \parallel^2 + \beta \parallel \frac{d^2\boldsymbol{u}(s)}{ds^2} \parallel^2 \tag{2}$$

$$+ E_{image}(\boldsymbol{u}(s)) + E_{con}(\boldsymbol{u}(s))ds \tag{3}$$

Here the first two terms constitute the internal energy term which are related to the tension and stiffness of the contour respectively. The image dependent energy is denoted by $E_{image}(\boldsymbol{u}(s))$. A typical example of $E_{image}(\boldsymbol{u}(s))$ is $-\|\nabla(G_\sigma * I)(\boldsymbol{u}(s))\|^2$, where G_σ is a Gaussian kernel with standard deviation σ and where $*$ denotes convolution. The curve minimizing the image dependent energy term only will

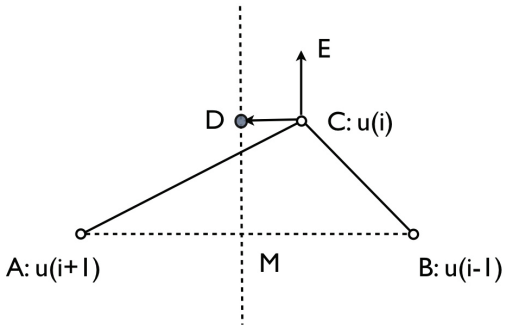

Fig. 4. Illustration of the inflating force and the proposed tangent force. Please see section 4.1 for a further explanation of the figure.

lock to the edges of the image. The last term $E_{con}(\boldsymbol{u}(s))$ represents an external constraint energy.

Using calculus of variations, one can minimize equation (5) by solving the related Euler-Lagrange equation. Usually the solution is obtained by an iterative approach where the curve deforms until convergence is obtained. Hence the nick-name snake.

A large number of improvements to the original snake formulation have been made. Space does not allow a review. However for the present approach the two most relevant improvement are due to [11] and [12]. In [11], the author suggested to add an additional inflating force to make the snake behave like an inflating balloon, see equation 3 . This overcomes the limitation of the original snake that it is difficult to initialize the contour.

$$F = k_1 * \overrightarrow{N}(s) \tag{4}$$

where $\overrightarrow{N}(s)$ denotes the normal unitary vector to the curve. k_1 is a scaling factor. This is equivalent to maximize the area Ω enclosed by the contour.

$$E = \int\int d\Omega \tag{5}$$

The inflating balloon method allow us to bootstrap the visual tracking algorithm without human intervention. In [13] it is reported that the use of an inflating force may cause loops of the contour. To prevent this [12] suggest to add a tangential redistribution term. This makes the contour control points more equally distributed along the contour. We will follow this approach. The numerical implementation of these two forces are shown in Fig.4.

B. A visual tracking method for extracting the weld pool boundary

To track the weld pool boundary revealed by image intensity edges we use the standard force $-\left\|\nabla(G_\sigma * I)(\boldsymbol{u}(s))\right\|^2$. In general the weld pool boundary changes slowly making it possible to use the final curve position from the previous frame as the initial position for the preceding frame. Often the image dependent force will be small at positions away from the true boundary. In particular, the gradient magnitude will be large at the arc light boundary. Especially when the arc is generated, the interference is very intensive making the arc light cover the true boundary of the weld pool and causing an instability of the tracking algorithms. Also, reflections may cause false edges to which the snake may falsely be attracted.

We therefore propose a periodically bootstrap strategy for the initialization of the active contours based on a binary classification of the frames as arc-on or arc-off. In Fig. 5, it is shown that arc-off frames and arc-on frames are categorized according to their intensities. Frames with an average intensity below a threshold will be regarded as arc-off frames. Otherwise, arc-on frames. This takes advantage of the fact that the arc is generated or disappears periodically during welding. Figure 6 shows the average intensity for a

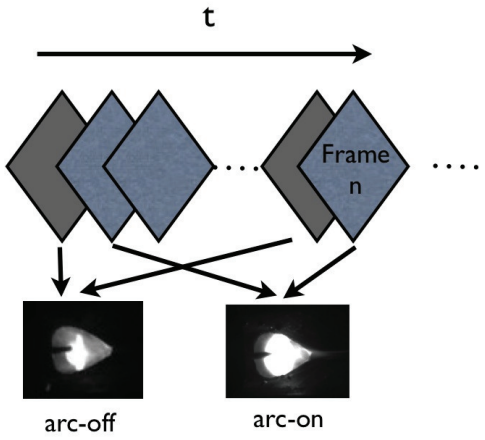

Fig. 5. The frames are categorized into two groups: arc-on frames and arc-off frames. This takes advantage of the fact that the arc is generated or disappeared periodically during welding.

sequence of frames. The arc-off frames marked by circles are solitude and spread more or less evenly across the sequence. This makes them useful for initialization frames. More important however, is that the true weld boundary is much more easily detectable in arc-off-frames.

In the case of arc-off frames, the arc light region is relatively small and will not cover the boundary of the weld pool. In this case, we threshold the image and use a modified inflating balloon to extract the weld pool boundary. Figure 7 shows the initial contour as a circle. The modified inflating balloon is then used to extract the weld pool boundary.

For arc-on frames, more intensive arc light can be observed, occasionally covering the weld pool boundary. We use an active contour without the inflating force and the tangent force to extract the weld pool boundary. In this case, we rely on the contour position from the previous frame as a good initial position. The pseudo-code of the proposed method can be found in Algorithm 1.

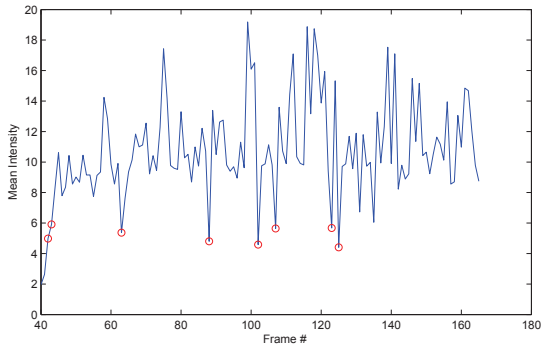

Fig. 6. This is a graphically illustration of categorizing frames into arc-off frames and arc-on frames. The arc-off frames are marked by circles. The curve shows the average intensity of all frames.

Fig. 7. This figure illustrates the initialization of inflating balloons in an arc-off frame. This is a binary image by thresholding the original frame. The black circle inside the white region represents the initial position of the inflating balloons.

V. Experimental Evaluation

A. Optimization of the Parameters

The parameters used in the proposed approach are summarized in Table I. The weights α and β regulate the tension and the stiffness of the active contours. The inflating force weight k balances the inflating force against the other forces. We optimize these parameters by trial and error.

B. Experiments

In order to evaluate the proposed machine vision system, several real-time demonstrations have been made. In these experiments, the welding process we used is short-arc MAG welding. The workpiece is v-groove structured steel. The

TABLE I

Parameters used in the proposed approach

Internal force weight : Tension	α	0.01
Internal force weight : Stiffness	β	0.01
Spacial step size	$\triangle s$	1
Temporal step size	$\triangle t$	0.01
The inflating force weight	k	0.002
Threshold for arc-on/off frame categorization	λ_1	6
Threshold for the arc-off frames	λ_2	30

Algorithm 1 : Weld Pool Boundary Tracking Algorithm

INPUT : A frame I

OUTPUT : A set of points describing the contour of the weld pool $P_i, i = 0, ..., N$

```
Check the frame type, arc-on or arc-off.
if I is an arc-off frame then
    Run InflatingBalloon to extract the weld pool boundary.
else
    if I is an arc-on frame then
        Run ActiveContours without an inflating force.
    end if
end if
```

TABLE II

Welding parameters

Wire-feed speed:	5.5 m/min
Wire diameter:	1.0 mm
Voltage :	14.9 V
Current:	$\sim$ 139 A
Shielding gas:	Argon(82%)/CO2(18%)

welding parameters used in these experiments are shown in Table II.

Fig. 8 shows several typical frames captured at a first layer welding. The weld pool boundaries were extracted in real time and marked by white curves. It can be seen that our vision system was able to track the weld pool boundaries accurately and stably in the presence of strong welding arc light. Specifically, Frame 63 was recognized as an arc-off frame. A modified inflating balloon was able to extract the boundary accurately. For the following arc-on frames, there were considerable arc light presented in the weld pool area. The active contours without the inflating force and the greedy tangent force would then start evolving from the initial curve given by the weld pool boundary extracted in arc-off frame. The results shows that this scheme performed very well. In frame 125, we had another arc-off frame. The procedure would start over again.

To further examine the ability to handle significantly different weld pools, experiments in a second layer welding have been carried out. The results were shown in Fig. 9. It can be seen that the proposed vision system succeeded in tracking the weld pool boundaries, even in the case that the arc-light covered the whole weld pool area, see frame 2.

VI. Conclusion

A low-cost machine vision system without external Illumination for directly weld pool sensing is proposed paving the way for a future closed-loop control system in arc welding. The main challenge of observing the weld pool directly is to overcome the interference of the high intensity arc light. We propose to use a bandpass filter combined with a neural density filter to filter out most of the arc light. The weld pool boundary was extracted using an active contour approach together with a regularly repeated initialization

process working on the arc-off frames only. On the vast majority of arc-on frames the needed amount of computational resources is limited. Thus, the system easily work real time. Finally, experiments demonstrated the feasibility of this vision system. For future works, visual features can be formed based on the analysis of the weld pool shape. We will realize an adaptive control system of the welding condition based on these visual features.

REFERENCES

[1] D. Brzakovic and D. Khani, "Weld pool edge detection for automated control of welding," *Robotics and Automation, IEEE Transactions on*, vol. 7, no. 3, pp. 397 –343, Jun. 1991.

[2] B. Abdullah, J. Smith, W. Lucas, J. Lucas, and M. Houghton, "A low-cost vision system for real-time monitoring of welding applications," in *14th Int. Conf. on the Joining of Materials and 5th Int. Conf. on Education in Welding*, Helsinger, Denmark, April 2007.

[3] D. Zhao, S. Chen, L. Wu, and Q. Chen, "Extraction of three-dimensional parameters for weld pool surface in pulsed gtaw with wire filler," *J. Manuf. Sci. Eng.*, vol. 125, no. 3, pp. 493–503, 2003.

[4] H. Song and Y. M. Zhang, "Measurement and analysis of three-dimensional specular gas tungsten arc weld pool surface," *Welding Journal*, vol. 87, pp. 85.s–95.s, 2008.

[5] C. Balfour, J. Smith, and A. AI-SHAMMA'A, "A novel edge feature correlation algorithm for real-time computer vision-based molten weld pool measurements," *Welding Journal*, vol. 85, no. 1, pp. 1.s–8.s, 2006.

[6] H. Luo, F. Lawrence, J. Wang, P. Mohanamurthy, A. Devanathan, X. Chen, and S. Chan, "Vision based gta weld pool sensing and control using neurofuzzy logic," Automation Technology Division, Singapore Institute of Manufacturing Technology, Tech. Rep. TR-00-11-AMP, 2000.

[7] H. Shen, J. Wu, T. Lin, and S. Chen, "Arc welding robot system with seam tracking and weld pool control based on passive vision," *The International Journal of Advanced Manufacturing Technology*, vol. 39, pp. 669–678.

[8] N. Otsu, "A threshold selection method from gray level histograms," *IEEE Trans. Systems, Man and Cybernetics*, vol. 9, pp. 62–66, Mar. 1979, minimize inter class variance.

[9] J. Canny, "A computational approach to edge detection," *IEEE Trans. Pattern Anal. Mach. Intell.*, vol. 8, no. 6, pp. 679–698, 1986.

[10] M. Kass, A. Witkin, and D. Terzopoulos, "Snakes: Active contour models," *International Journal of Computer Vision*, vol. 1, no. 4, pp. 321–331, 1988.

[11] L. D. Cohen, "On active contour models and balloons," *CVGIP: Image Underst.*, vol. 53, no. 2, pp. 211–218, 1991.

[12] H. Delingette and J. Montagnat, "Shape and topology constraints on parametric active contours," *Computer Vision and Image Understanding*, vol. 83, pp. 140–171, 2000.

[13] V. Srikrishnan and S. Chaudhuri, "Stabilization of parametric active contours using a tangential redistribution term," *Trans. Img. Proc.*, vol. 18, pp. 1859–1872, August 2009.

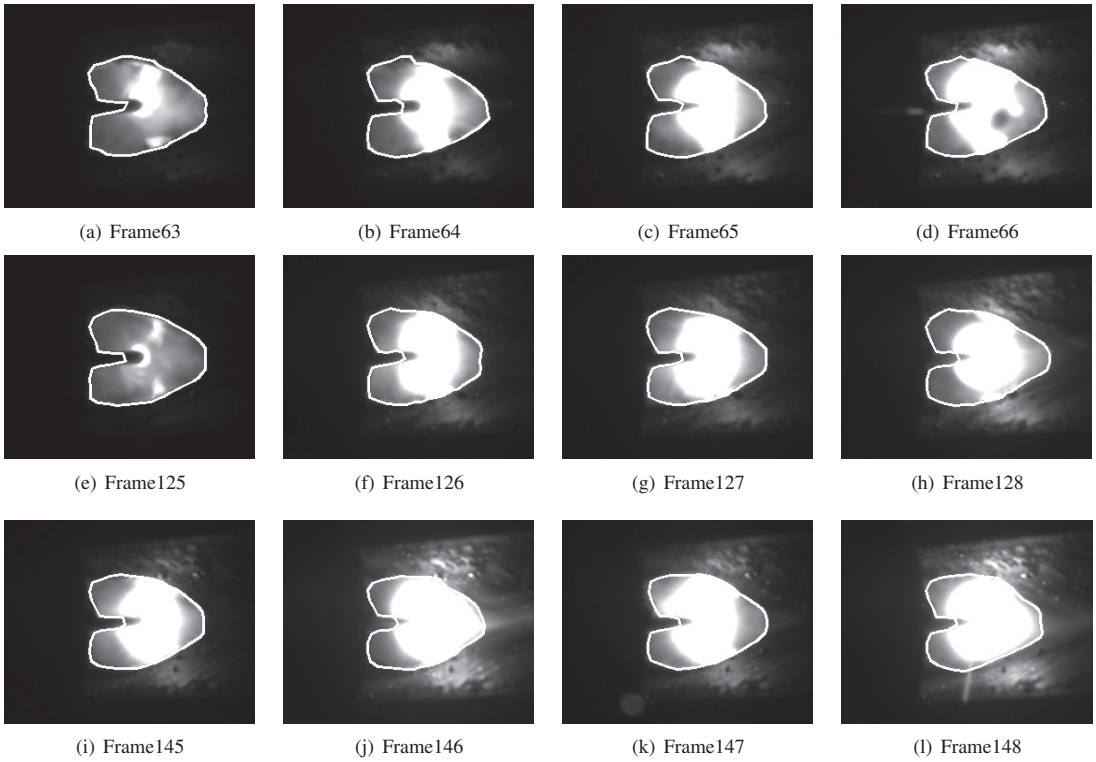

(a) Frame63 (b) Frame64 (c) Frame65 (d) Frame66

(e) Frame125 (f) Frame126 (g) Frame127 (h) Frame128

(i) Frame145 (j) Frame146 (k) Frame147 (l) Frame148

Fig. 8. Experiment 1. Here the tracking results of weld pool boundaries in the case of a first layer welding were shown.

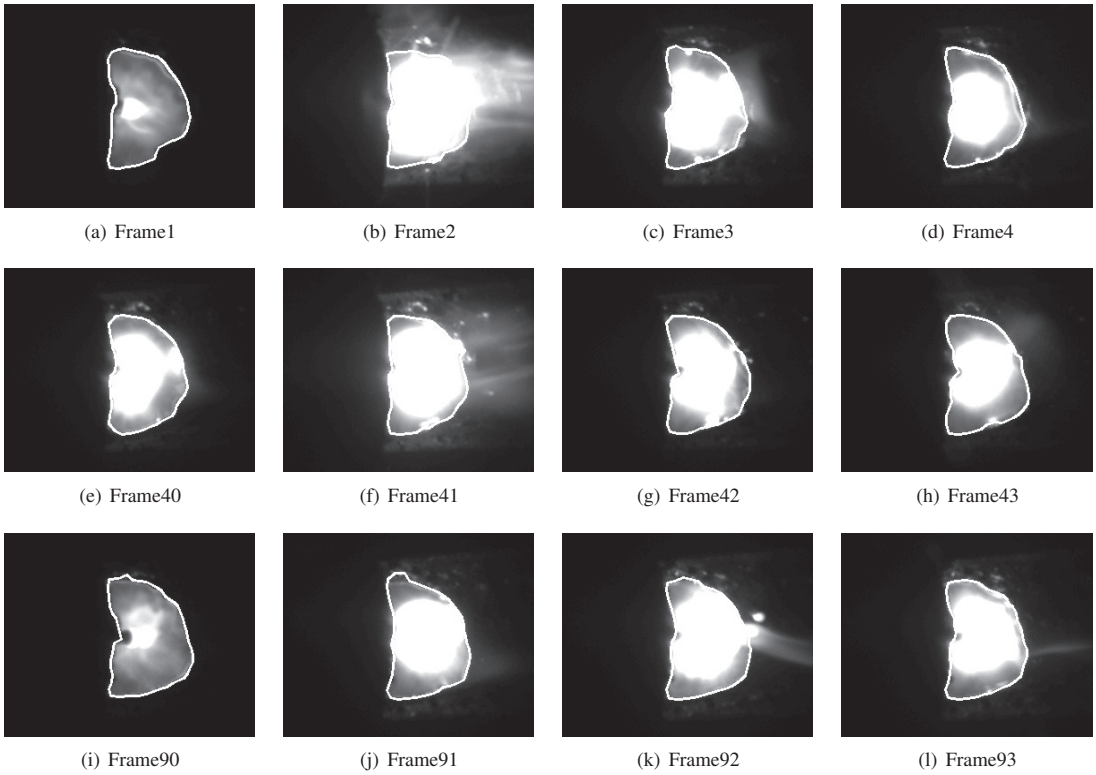

(a) Frame1 (b) Frame2 (c) Frame3 (d) Frame4

(e) Frame40 (f) Frame41 (g) Frame42 (h) Frame43

(i) Frame90 (j) Frame91 (k) Frame92 (l) Frame93

Fig. 9. Experiment 2. This figure shows tracking results of weld pool boundaries in the case of a second layer welding. It can be seen that the weld pool boundaries are quite different from the first layer welding presented in experiment 1.